BOREAL ENVIRONMENT RESEARCH 31: 111–124
ISSN 1797-2469 (online)
© 2026
Helsinki 6 October 2026

Yearly Ozone Uptake Accumulation Periods for Swedish Forest Trees and Agricultural Crops

Per Erik Karlsson[1)], Gunilla Pihl Karlsson[1)], Helena Danielsson[1)] and Håkan Pleijel[2)]

[1)] *IVL Swedish Environmental Research Institute, P.O. Box 53021, SE-40014 Göteborg, Sweden*
[2)] *University of Gothenburg, Biological and Environmental Sciences, P.O. Box 463, SE-40530 Göteborg, Sweden*
**corresponding author's e-mail: pererik.karlsson@ivl.se*

Received 27 Feb. 2026, final version received 24 Aug. 2026, accepted 24 Aug. 2026

Karlsson P.E., Karlsson G.P., Danielsson H. & Pleijel H. 2026: Yearly Ozone Uptake Accumulation Periods for Swedish Forest Trees and Agricultural Crops. *Boreal Env. Res.* 31: 111–124.

Ground-level ozone (O_3) impacts on vegetation are estimated based on the accumulated O_3 taken up to the leaf interior during one growing season, i.e. the Phytotoxic Ozone Dose, POD. Determination of POD is dependent on estimates of the yearly time periods when stomata may be open allowing ozone uptake, i.e. the ozone accumulation periods (O_3AP). An improved methodology was developed for calculating O_3AP for coniferous and deciduous tree species, wheat, and potato for Sweden. For coniferous trees the start of O_3AP was estimated as when the 24h mean air temperature exceeded a threshold value. For deciduous trees, the start of O_3AP was based on the accumulated temperature sum above 5°C. For wheat, a relationship between the timing of anthesis and site latitude was suggested, with separate parametrisation for winter and spring wheat, respectively. For potatoes, a relationship between the timing of tuber initiation and the site latitude was determined.

Introduction

Tropospheric, ground-level ozone (O_3) is a toxic, secondary air pollutant that negatively affects vegetation (Emberson 2020). O_3 is also a significant greenhouse gas. Ground-level O_3 is formed in the lower troposphere in photochemical reactions, driven by the energy from solar radiation, from the precursors nitrogen oxides (NO_x), volatile organic compounds (VOCs including CH_4) and carbon monoxide (CO). These O_3 precursors are transported long distances in the atmosphere, making ground-level O_3 a transboundary, large-scale air pollution problem.

The toxic effects of O_3 on vegetation depend on leaf O_3 uptake mechanisms (Mills *et al.* 2011). To cause toxic effects, O_3 must be absorbed into the leaf interior through the stomata, the numerous tiny pores on leaves that control plant gas exchange. Hence, the severity of O_3 effects on vegetation is determined by the accumulated leaf O_3 uptake, i.e. the Phytotoxic Ozone Dose over a threshold Y calculated for SPECific plant species, POD_YSPEC (Mills *et al.* 2011). Environmental risk indices for ozone induced damage based on POD_YSPEC are more closely related with observed impacts on vegetation as compared with concentration-based indices like AOT40 (Karlsson *et al.* 2007; Mills *et al.* 2011; Pleijel *et al.* 2022).

POD_YSPEC should be accumulated during yearly O_3 accumulation periods (O_3AP), which

Editor in charge of this article: Veli-Matti Kerminen
https://doi.org/10.60910/ber2026.bjng-4520

to some extent coincide with the growing seasons. However, for agricultural crops O_3AP also depends on specific aspects of plant development, which in turn depends on agricultural practices and weather patterns. In annual crops, the sensitivity to O_3 becomes larger as the plants enter the reproductive stage (Pleijel *et al.* 1998; Soja *et al.* 2000). Hence, estimates of the POD$_Y$SPEC depend on the atmospheric O_3 concentrations next to the leaves, the meteorological and growth conditions, on plant developmental stages as well as on other properties, such as the species-specific sensitivity to O_3.

The current methodology for calculating POD$_Y$SPEC, as specified in the LRTAP Mapping Manual (UNECE 2017), is based on generalized estimates mainly basis on the geographical location that might not fully capture Swedish environmental conditions, especially regarding the plant phenological processes such as recovery from winter dormancy in trees.

The aim of this study was to suggest improvements for the phenology functions used for estimating O_3AP for some important Swedish plant species, by making use of micro-meteorological canopy gas exchange measurements, utilizing extensive phenological observations and using national agricultural statistics for Sweden. Norway spruce (*Picea abies*) and Silver birch (*Betula pendula*) are common tree species in Sweden. Wheat (*Triticum aestivum*) is a widely grown and intensively studied agricultural crop in Sweden which has been shown to be highly sensitive to O_3 (Pleijel *et al.* 2018). Potato (*Solanum tuberosum*) is another important crop known to be negatively affected by O_3 (Vandermeiren *et al.* 2005).

Material and methods

General methods for estimating PODySPEC for vegetation

The POD$_Y$SPEC is calculated for different plant species or plant functional types according to methods that are described in detail in the Mapping Manual (UNECE 2017). POD$_Y$SPEC is the ozone flux through stomata, F_{st}, accumulated over a threshold value, Y, over one growing season. The general equation for estimating F_{st} is given by:

$$F_{st} = g_{st} \times \mu_{st} \times r_c / (r_b + r_c), \quad \text{(Eq. 1)}$$

where F_{st} is the ozone flux through stomata in nmol m^{-2} (projected leaf area, PLA) s^{-1}, μ_{st} is the ozone concentration at canopy height in nmol m^{-3} and g_{st} is the stomatal conductance for ozone in m s^{-1}. The component r_c / $r_c + r_b$ accounts for other resistances for ozone diffusion from air to leaf, besides g_{st}. r_c is the leaf surface resistance (s m^{-1}), and r_b is the quasi-laminar resistance (s m^{-1}).

The calculation of the stomatal conductance, g_{st}, follows the multiplicative algorithm suggested by Emberson *et al.* (2000):

$$g_{st} = g_{max} \times \min(f_{phen}, f_{O3}) \times f_{light} \times \max(f_{min}, (f_{temp} \times f_{VPD} \times f_{SW})), \quad \text{(Eq. 2)}$$

where the unit for g_{st} is mmol O_3 m^{-2} PLA s^{-1}), g_{max} is the maximum stomatal conductance for the specific plant species in mmol O_3 m^{-2} PLA s^{-1}. f_{min} is the minimum stomatal conductance during daytime, as a fraction of g_{max}. The different factors ("f-functions") limiting the stomatal conductance, are governed by physical and meteorological conditions and can have values between 0 and 1. f_{temp} represents the limitation by air temperature, f_{light} by solar radiation, the f_{VPD} by air water vapor pressure deficit and f_{SW} by soil water availability. The limitation of stomatal conductance by phenology, such as release of dormancy, growing season or flowering is represented by the f_{phen}. The modification of stomatal conductance by an accumulated impact of stomatal ozone uptake is represented by the f_{O3}. However, the f_{O3} function is not used for forest trees.

Methods for estimating f_{phen} for trees

The general function that describes how the phenology will limit the estimated potential stomatal conductance during O_3AP for northern and central European tree species, f_{phen}, is described in Fig. 1. A_{start} and A_{end} are the start and end of the O_3AP respectively. f_{phen1} and f_{phen4} are the time periods describing the duration from one phenological stage to another.

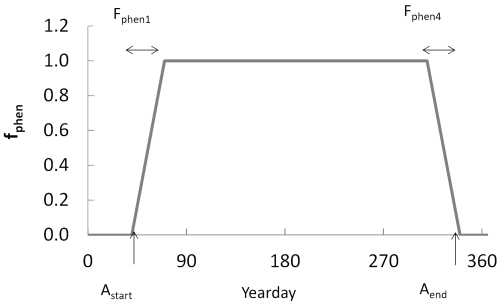

Fig 1. The f_{phen} function describes how the phenology limits the estimated potential stomatal ozone uptake during O_3AP during different parts of the year for northern and central European tree species. At f_{phen} = 1 the phenology does not limit stomatal ozone uptake. The day of year after the winter dormancy period when the O_3AP of a certain tree species begins is called "A_{start}" and the day of year during autumn when O_3AP ends is called "A_{end}". The duration from f_{phen} = 0 at "A_{start}" to reach f_{phen} = 1 is called f_{phen1}. The number of days it takes from f_{phen} = 1 to f_{phen} = 0 before "A_{end}" is called f_{phen4}. The different abbreviations and the figure are simplified from the Mapping Manual (UNECE 2017).

The term "start of the growing season (SGS)", is generally used as the time when the vegetation in boreal and temperate climate zones starts its physiological activity after a winter dormancy period. In many cases the start of O_3AP for trees has been set equal to the SGS. However, SGS is a more general term, including physiological processes such as growth, photosynthesis recovery after dormancy etc. O_3AP more specifically has to comply with the period of the year when O_3 can be taken up by the stomata, i.e. when the stomatal conductance potentially may be higher than zero.

In the UNECE Mapping Manual (UNECE 2017), parameterizations for Norway spruce and Birch are used to represent coniferous and deciduous boreal forests. The same principle was applied also in our study.

Specific methods for estimating f_{phen} for boreal coniferous tree species

In the methods currently suggested in the Mapping Manual for Norway spruce in the boreal region, A_{start} is estimated using a "Latitude model" where A_{start} occurs at year day 105 at latitude 50°N, and A_{start} will alter by 1.5 days per degree latitude earlier on moving south and later moving north. A_{end} is estimated to occur on year day 297 at latitude 50°N, and A_{end} will change two days per degree latitude earlier on moving north and later moving south.

The approach in the present study was to determine O_3AP for coniferous tree species based on the period when forest canopy gas exchange can be detected. For this purpose, we used hourly data for net ecosystem exchange of CO_2 for forest canopies (NEE) from the Integrated Carbon Observation System (ICOS)-Sweden at three different sites across Sweden for four years with relatively complete datasets, 2014–2017 (http://www.icos-sweden.se). The sites were Hyltemossa in southern Sweden, Norunda in south-central and Svartberget in north Sweden. (Fig. 2).

A consistent negative value for NEE, i.e. a net uptake of CO_2 from the atmosphere to the forest stand, indicated that stand photosynthesis rates were higher than stand respiration rates. Rates of photosynthesis above zero require the stomata to be at least partially open, which in turn would allow for ozone uptake into the leaf interior. Hence, the start of O_3AP at each site and each year was defined as the time of year when the mean NEE during mid-day, 10:00–13:59, was below –1.0 μmol m^{-2} s^{-1} for five consecutive days. The last value for day-of-year of these five days was used in further analysis. The date for the start of O_3AP for the three sites was correlated with the date when the 24 h mean air temperatures for five consecutive days exceeded a temperature threshold value at each site the same year. The same threshold value could not be applied for all sites due to the substantially different climate conditions in northern, compared to southern Sweden. Instead, a threshold of 1.5°C had to be used for Hyltemossa and Norunda and a threshold of 0°C was used for the northernmost site, Svartberget. Furthermore, for the southernmost site, Hyltemossa, a restriction had to be made that the start of O_3SP could not occur before 1 February. Thus, the estimated start of O_3AP will vary over the years due to weather conditions. The daily 24h mean temperatures were obtained from the Swedish Meteorological and Hydrological Institute, SMHI.

The end of O_3AP was estimated as the DOY for last day of the five-day period when the NEE

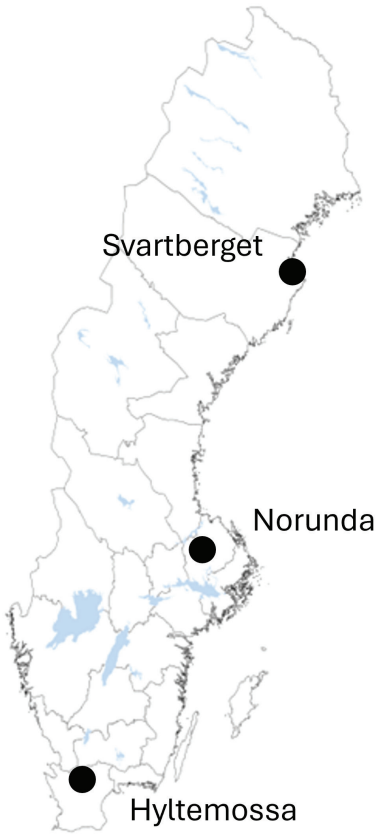

Fig 2. A map showing the three sites in Sweden with micro-meteorological measurements of "Net Ecosystem Exchange", NEE, of CO_2 within ICOS-Sweden (http://www.icos-sweden.se) as well as showing the location of the 21 different counties of Sweden, used in the analysis for the agricultural crops. Hyltemossa (56° 10′N, 13° 42′E, 115 m a.s.l.) is positioned in southernmost Sweden, nemoral zone. Svartberget (64°15′N, 19°46′E, 270 m a.s.l.) is positioned in north Sweden, boreal zone. Norunda (60°05'N, 17°29'E, 46 m a.s.l.) is positioned in the transition between the boreal and nemoral zones.

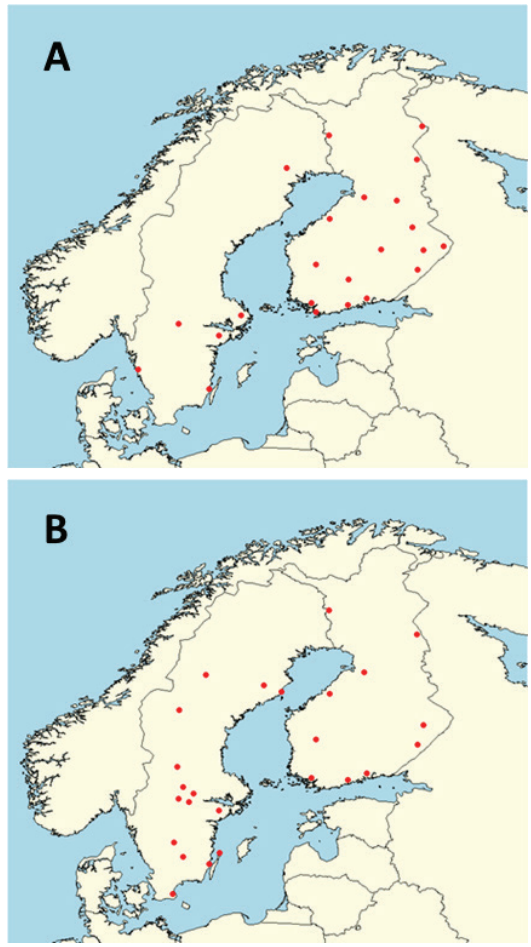

Fig 3. Maps over sites where phenological observations used in this study were made to determine the dates for budburst (**A**) and the dates for the start of autumn coloration (**B**) for Birch (*Betula pendula* and *B. pubescens*) in Sweden and Finland. Source for Finnish data: Dr Eero Kubin, Finnish Forest Research Institute, Muhos Research Unit. Source for Swedish data: Dr Kjell Bolmgren.

no longer was below –1.0 μmol m^{-2} s^{-1} during five consecutive days. This date was correlated with the latitude for the different sites and thus kept constant between years.

Specific methods for boreal deciduous tree species

For deciduous trees there are obvious, visible signs for the start and end of the O_3AP, since the gas exchange of the leaves can be assumed to be correlated with leaf expansion after budbreak (Breda and Granier 1996). The O_3AP for Birch was estimated based on phenological observation data from Finland and Sweden (Fig. 3), obtained from the Pan-European Phenology Network (PEP725, Templ *et al.* 2018) and the Swedish Phenology Network (data supplied by Dr Kjell Bolmgren). The classification "bbch 10" was used to determine the date for budburst while "bbch 94" was used for the date for the start of autumn coloration. Data for both Silver birch, *Betula pendula,* and Downy birch, *B. pubescens*,

were used, without separation between these two species.

The analysis of the time for budburst was based on data from 17 sites in Finland, with no more than one year missing data for the period 1997–2011. Furthermore, data was used for six sites in Sweden with no more than one year with missing data for the period 2013–2016. The analysis of the time for the start of autumn coloration was based on data from ten sites in Finland, with no more than one year with missing data for the period 2008–2013 and data from 15 sites in Sweden with no more than one year missing data for the period 2010–2015.

The start of O_3AP for deciduous tree species was determined as the time for budburst, which in turn was correlated with the accumulated 24-h mean air temperature sum above 5°C from 1 January of the specific year exceeding 45-degree days. The 24-h mean air temperatures for Finland were obtained from the MESAN system (Häggmark *et al.* 2000). The 24-h mean air temperatures for Swedish sites were obtained from SMHI.

The end of O_3AP for deciduous tree species remains difficult to refine due to limited knowledge of the physiological mechanisms governing autumn leaf senescence (see Discussion section). The current methodologies in the Mapping Manual (UNECE 2017) that rely on site latitude-based estimates, were maintained in this study due to the lack of more accurate physiological models.

Specific methods for agricultural crops

For annual crops, like wheat and potato, the O_3APs as specified in the Mapping Manual (UNECE 2017) are based on temperature sums accumulated before and after critical phenological stages, for wheat anthesis ("flowering"; Grünhage *et al.* 2012) and for potato tuber initiation (Pleijel *et al.* 2007). To adapt methods for estimating POD to regional conditions, the task is to provide accurate estimates for the date of anthesis and tuber initiation, respectively, for different areas where wheat and potato are cultivated. To exemplify such methods, the dates of anthesis and tuber initiation were identified using Swedish agricultural statistics from the Swedish Board of Agriculture, Forecast and Warning of the Regional Plant Protection Centres, for the 21 different counties in Sweden (Fig. 2) covering 2000–2025 for wheat and 2004–2025 for potato. Information was essentially complete for wheat while for potato temporal and spatial coverage of the data was limited. For wheat, the critical phenological stage used to identify O_3AP was based on mid-anthesis (flowering midpoint), which was determined by averaging the day of year (DOY) corresponding to stages DC64-66 in the decimal growth scale (Zadoks *et al.* 1974) over all years and for each county. The data obtained was tested in relation to the latitude model for mid-anthesis suggested by the Mapping Manual (UNECE 2017):

$$\text{Mid-anthesis} = 2.57 \times \text{latitude} + 40. \quad \text{(Eq. 3)}$$

Mid-anthesis is defined by the numerical day number of the year when it occurs, latitude is expressed as the decimal latitude, degrees N. According to the manual, this equation is supposed to be applied for both spring- and winter wheat. We used the average latitude of each of the 21 counties which ranged from 55.95° to 66.93°. Furthermore, we tested to reparametrize the latitude function (Eq. 3) by minimizing the sum of squared differences between observed and modelled date of anthesis (least square method) for the data set of this study.

For potato, a similar scale (BBHC) was used, where DC39-41 represents tuber initiation (Meier 2001). The Mapping Manual (UNECE 2017) does not suggest a latitude model (or any other model) to assess the timing of planting or tuber initiation for potato; this is assumed to be based on local information. Thus, we limited the analysis here to study the DOYs of planting and of tuber initiation, in relation to latitude based on the Swedish counties for which data were available.

Results

Coniferous tree species

There was, for the three sites analyzed with data for coniferous tree species, a relatively strong relation between the DOY for the onset of a five-

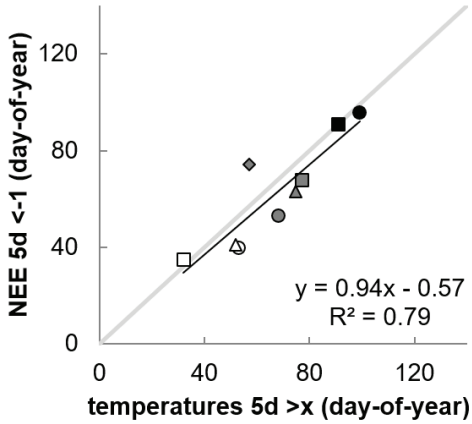

Fig 4. The correlation between the day-of-year for the start of NEE, and the day-of-year for 24h mean air temperatures exceeding the different thresholds for three ICOS sites. On the y-axis is shown the day-of-year when the daytime CO_2 NEE decreased below –1 μmol m^{-2} s^{-1} for five consecutive days. On the x-axis is shown the corresponding day-of-year when the 24h air temperatures exceeded a threshold value for five consecutive days. The threshold values were 1.5°C for the southern sites Hyltemossa (white symbols) and Norunda (grey symbols) and 0°C for the northern site Svartberget (black symbols). Data were from four different years, 2014 (diamonds), 2015 (circles), 2016 (squares) and 2017 (triangles). The solid grey line shows the 1:1 relationship.

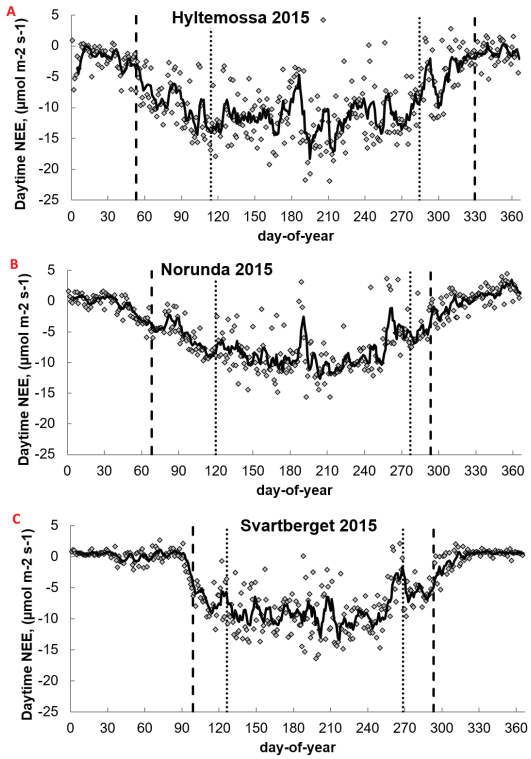

Fig 5. Daily values for Net Ecosystem Exchange of CO_2 (NEE) as mean values for the middle of the day (10:00–13:59) for the year 2015 for Hyltemossa (**A**), Norunda (**B**) and Svartberget (**C**) plotted versus day-of-year. A solid black line indicates the running five-day mean values. Vertical broken black lines indicate the Astart and Aend estimated with the new method suggested in this study based on 24h mean air temperatures. Vertical dotted black lines indicate the A_{start} and A_{end} estimated with the current methods in the Mapping Manual.

day permanent negative NEE and the five-day 24h mean air temperatures exceeding the different thresholds, with a R^2 of 0.79 (Fig. 4). The mean values across years for the start of O_3AP at the different sites ranged from DOY 54 in southern Sweden DOY 83 for the most northern sites. As a mean value across the years, the A_{start} occurred 69, 47 and 27 days earlier with the new method developed in this study, as compared to the original, latitude-based method in the Mapping Manual, for Hyltemossa, Norunda and Svartberget,

At the site Hyltemossa, in southernmost Sweden, there was no period during the winters 2015/16 and 2016/17 when the daily NEE was not below zero, while this was the case for the winter 2014/15. These results are difficult to handle statistically. It was suggested that A_{start} at any site could not occur before 1 February. The significance of this assumption is small since the O_3 concentrations are generally very low in January in northern Europe.

An example for the daily daytime values for NEE for the year 2015, a year when a relatively complete dataset was available for all three sites, plotted against the DOY, is shown in Fig. 5. Also shown is the estimated A_{start} and A_{end} estimated with the new methods described in this study, together with the A_{start} and A_{end} as calculated with the current, latitude-based methods described in the Mapping Manual. The corresponding figures for the remaining years are shown in the Supplementary Information (SI), Figs. S1, S2 and S3.

The new method to estimate A_{start} and A_{end} suggested in this study was far more accurate, compared to the current method from the Mapping Manual (UNECE 2017). Hence, the revised

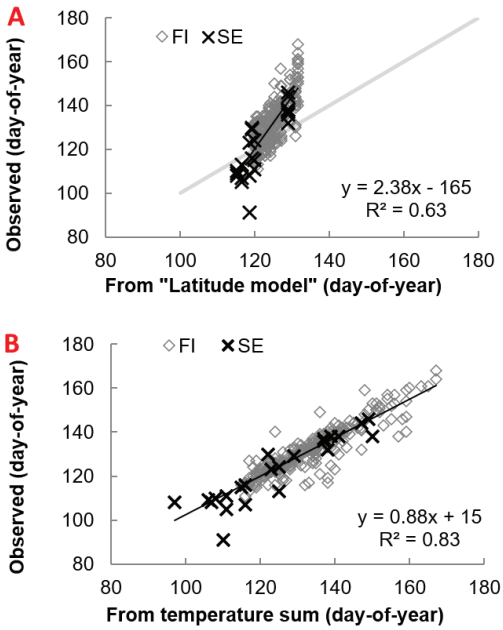

Fig 6. A comparison of the prediction of the time for budburst (day-of-year) for Birch in Sweden and Finland, compared to observed time for budburst, based on the currently used method in the Mapping Manual (UNECE 2017), i.e. the "Latitude model" (**A**), and based on the method developed in this study, based on the accumulated air temperature sum since 1 January, (**B**). In the latter model budburst is assumed to occur when the 24h air temperature sum exceed 45 degree-days. The analysis is based on phenology observations from Sweden (SE) and Finland (FI).

methodology for Norway spruce significantly improved the accuracy of O_3AP estimates for Swedish climate conditions, incorporating previously underestimated ozone exposure during early spring.

One possible method to estimate A_{end} would be to determine the last five-day period of the year when the NEE was below –1,0 µmol m^{-2} s^{-1} and relate that the last five-day period when the 24-h air temperatures exceeded the respective threshold. However, such relation could not be established (data not shown). The current method used in the Mapping Manual to establish A_{end}, based on the "Latitude model", seem to result in a value for day-of-year that occur too early in the year (Fig. 5 and SI Figs. S1, S2 and S3). Instead, the estimated time of year for the last five-day period of the year when the NEE at the three sites was below –1,0 µmol m^{-2} s^{-1} was related to the latitude for the three sites (see SI Fig. S4). The correlation coefficient was weak, but we suggest that this correlation with the latitude is more relevant for northern coniferous forests, compared to the current methods described in the Mapping Manual (UNECE 2017).

Data such as those shown in Fig. 5 could not be used to define f_{phen1} and f_{phen4}, i.e. the time from A_{start} until maximum f_{phen} and the time from maximum f_{phen} until A_{end}, respectively, since the day-time NEE will, besides day of year, depend on many different environmental conditions. In the absence of new information, we suggest that the values for f_{phen1} and f_{phen4} that are suggested in the Mapping Manual, 20 and 30 days, respectively, remain for the parameterization for f_{phen} for Norway spruce in northern Europe.

Deciduous tree species

There was a relatively weak correlation between the DOY for the observed budburst of Birch in Sweden and Finland and the latitude of the site (Fig. 6a), i.e. the method to estimate A_{start} suggested in the Mapping Manual (UNECE 2017).

The relation between the predicted DOY for budburst estimated with the new method developed in this study, i.e. to use the DOY when the accumulated air temperature sums above 5°C exceeded 45 degree-days, and the observed values for DOY for budburst are shown in Fig. 6b. The correlation coefficient was much higher compared to the results with the "latitude model", and the slope was 0.9. Hence, the new method developed in this study provided a more accurate representation of interannual variability in budburst for Birch in Sweden and Finland, also improving the model's responsiveness to climate change.

During 2000–2006 maps were published for every 3rd day showing the current state of budburst of Birch in many sites across Finland. Based on this information we calculated the time between first observations of budburst and fully expanded leaves at different latitudes in Finland (Fig. 7).

The time between the start of budburst and fully expanded leaves for Birch in southern Finland varied between six and 52 days

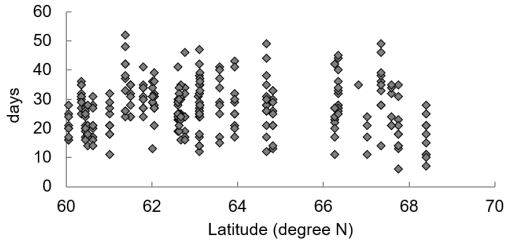

Fig 7. Estimate of the number of days between first observations of budburst and fully expanded leaves for Birch at sites with different latitudes in Finland 1997–2006. The value used in the Mapping Manual (UNECE 2017) for f_{phen1} for deciduous trees is 20 days. The maps with information about the state of budburst were obtained from Eero Kubin, Finnish Forest Research Institute, Muhos Research Unit.

(Fig. 7), depending on year and site latitude. In the southern parts, it varied between 16 and 28 days. In the Mapping Manual (UNECE 2017), a value of 20 days is used for f_{phen1} for deciduous trees in northern Europe. We suggest that the value for f_{phen1} of 20 days should remain for deciduous trees in Sweden and Finland.

The start of autumn coloration represents the time defined as A_{end} subtracted by f_{phen4}. The timing of the start of autumn coloration in Birch in relation to the site latitude was analysed based on the data from the Swedish and Finnish phenological networks (see SI Fig. S5). The relation between the start of autumn coloration and the site latitude was weak and the time for autumn coloration occurred almost simultaneously at all sites, independent of latitude. The relation with latitude was even weaker compared to what was predicted from the "latitude model" currently used in the Mapping Manual (UNECE 2017).

The number of days between the start of the leaf autumn coloration and the leaf detachment for birch observed at different sites in the Finnish phenological network 1997–2006 is shown in the SI, Fig. S6. There was a large variation in the number of days between the start of the leaf autumn coloration and the leaf detachment, between six and 63 days, depending on year and latitude. For southern latitudes, the variation was between 14 and 38 days, when two outlier values were excluded. The analysis of A_{end} and A_{phen4} for birch in Sweden and Finland described above did not provide a solid basis to suggest a revision of the current methods used in the Mapping

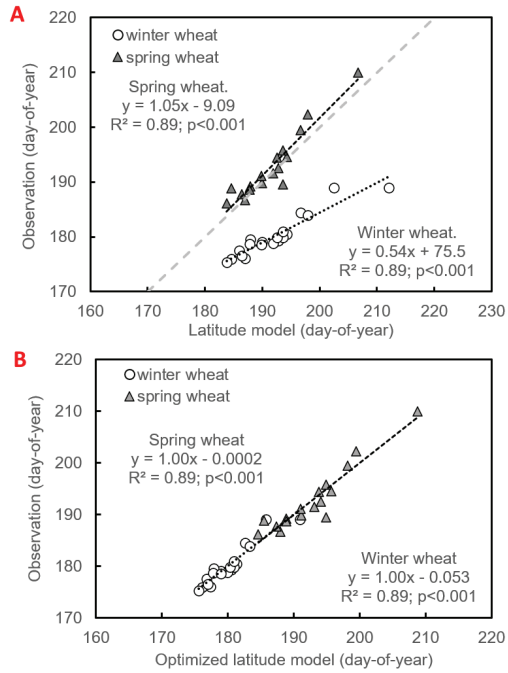

Fig 8. (**A**), Observed average day of year (DOY) of anthesis for different Swedish counties in relation to the DOY estimated with the latitude model of the Mapping Manual (UNECE, 2017) for spring and winter wheat. (**B**), As in **A**) but with the latitude model optimized for spring and winter wheat separately for the data set of this study.

Manual (UNECE 2017). Therefore, we suggest that the current methods should remain, using the value 20 days for f_{phen4}.

Agricultural crops

The relationships between the observed average DOY for mid anthesis for the different Swedish counties and those estimated by the latitude model in the Mapping Manual (UNECE 2017, Eq. 3) for the same sites are presented in Fig. 8a. It was clear that the latitude function worked very well for spring wheat with only a small deviation from the 1:1 relationship. For winter wheat, however, the latitude model overestimated the DOY by 10–20 days, with the larger deviations at higher latitudes. The correlation between estimated and observed DOY of anthesis was, however, strong, showing that the latitude is a strong predictor for day of anthesis

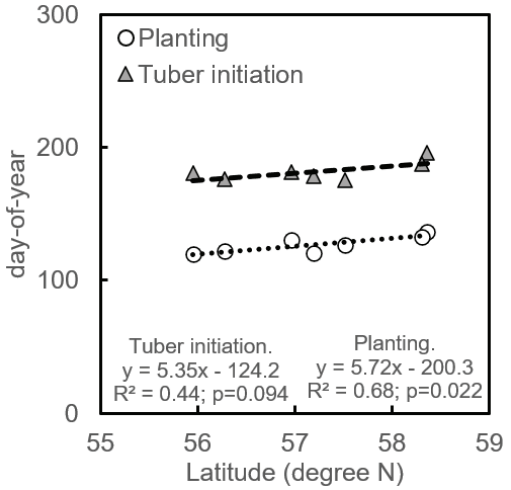

Fig 9. Day of year (DOY) of planting and tuber initiation in relation to latitude for seven Swedish counties with substantial potato production.

also in winter wheat, although the calibration of the latitude function of the Mapping Manual (UNECE 2017) resulted in a substantial systematic bias.

By optimizing the latitude function separately for spring wheat and winter wheat based on the observation data set of this study and using the least square method, the following relationships were obtained:

$$\text{Spring wheat: DOY of Mid-anthesis} = 2.71 \times \text{latitude} + 33.1 \quad \text{(Eq. 4)}$$

$$\text{Winter wheat: DOY of Mid-anthesis} = 1.40 \times \text{latitude} + 97.3 \quad \text{(Eq. 5)}$$

Mid-anthesis is defined by the numerical day number of the year when it occurs, latitude is expressed as the decimal latitude, degrees N. When applying these functions (Fig. 8b) the relationship between observed and modelled DOY for anthesis did not change much for spring wheat although an improvement was made, while a considerable change was obtained for winter wheat, now with only small deviations from the hypothetical 1:1-relationship between observed and modelled DOYs for anthesis in the counties.

The relationships of DOYs for planting and tuber initiation for potato with latitude were consistent over the limited range of counties for which data were available (Fig. 9). Relations were weakly positive and statistically significant only in the case of DOY of planting ($p = 0.02$). However, the relation with tuber initiation was close to significant with $p = 0.094$. The number of days between planting and tuber initiation was on average 54 ± 4 (SD), i.e. between seven and eight weeks and with just a small variation between counties.

Discussion

O_3AP for coniferous forests

Obviously, there are no visible, macroscopic indicators that can be used for phenological observations of the start of needle general physiological activity of evergreen coniferous tree species, besides budburst and shoot elongation. Instead, analysis of the timing of the start of the general physiological activity had to rely on different forest ecosystem measurements, such as measurements of net ecosystem exchange of CO_2 (NEE).

Tanja *et al.* (2003) suggested, based on micrometeorological measurements of NEE, that the start of the growing season for boreal forests could be estimated as when the 24h mean air temperatures exceeded 4.7°C for five consecutive days. However, Lagergren *et al*. (2008) analysed micrometeorological measurements from forests in Finland, Sweden and Denmark and showed that the time of year when the difference between NEE during day- and nighttime reached a level of at least 5% of the maximal difference during the year occurred much earlier during the year compared to when the 24h mean air temperatures exceeded 4.7°C. Wallin *et al.* (2013) measured photosynthesis of 40-year-old Norway spruce with a branch cuvette system during several years at Flakaliden, which is close to the site Svartberget (Fig. 2). The current method used in the Mapping Manual for boreal coniferous forests based on the site latitude results in a value for the start of growing season at Flakaliden of DOY 126. However, it was obvious from the photosynthesis measurements that the photosynthesis of the spruce trees started much ear-

lier, well before DOY 90. Walther *et al.* (2013) assessed photosynthesis of northern evergreen needleleaf forest based on satellite measurements of sun-induced chlorophyll fluorescence (SIF). They concluded that on average, the photosynthetic spring recovery as signalled by SIF occurs as soon as air temperatures exceeded 2–3°C.

Thus, the results obtained in the present study, that the forest canopy gas exchange will start when the 24h mean air temperatures consistently exceed a threshold slightly above freezing temperatures, are consistent with earlier results reported in the scientific literature. Correct estimates of A_{start} for northern coniferous forests are particularly important since ozone concentrations may be relatively high at northern latitudes during early spring (Klingberg *et al.* 2019).

O_3AP for deciduous forests

Leaf budburst of deciduous forests during spring, as well as the start of leaf autumn coloration during autumn, is controlled by a combination of air temperatures and daylength (Fu *et al.* 2018; Kloos *et al.* 2024). The physiological mechanisms behind budburst and the start of autumn leaf coloration are not well known and may vary between different tree species (Flynn and Wolkovich 2018). Daylength has a large influence on the timing of the budburst of Beech (Zohner and Renner 2015). For Birch the between-year variation for the timing of budburst is relatively large (Poikolainen *et al.* 2016) indicating the air temperatures may have a large influence. In contrast, the timing of autumn leaf coloration for Birch in Finland has remained almost constant in the southern boreal zones of Finland, whereas it has advanced in the middle northern boreal zones (Poikolainen *et al.* 2016).

In the present study, the timing of the budburst of Birch was estimated based on phenological observations in Finland and Sweden as when the 24h mean air temperatures accumulated above 5°C since the beginning of the year exceeded a temperature sum of 45 degree-days. In a previous study young Birch plants of different clones were planted at different sites in Finland and it was found that bud burst could be predicted from the temperature accumulation with base temperatures between +5 and –2°C (Rousi and Pusenius 2005). The clones differed in their temperature requirements for bud burst, indicating a genetic basis for determination of bud burst.

The start of autumn leaf coloration and hence the onset of winter dormancy is mainly controlled by daylength (Jiang *et al.* 2022). However, the role of the daylength can be influenced by air temperatures through different interactions (Estiarte and Penuelas 2015; Gill *et al.* 2015; Jiang *et al.* 2022). Also, local meteorological parameters may influence the start of leaf coloration such as drought, strong winds and the number of solar hours (Liu *et al.* 2016). Keskitalo *et al.* (2005) studied the process of autumn leaf coloration of mature trees of Aspen, *Populus tremula*, in Umeå, close to the site Svartberget (Fig. 2). They concluded that the autumn leaf coloration of Aspen was initiated by daylength. Liu *et al.* (2016) analysed what they called "end-of-season, EOS" in north China based on satellite and suggested a relatively complicated model to predict EOS. They suggested that air temperatures during summer months had a large influence on EOS. They suggested that it may be possible to use the mean air temperatures during 1–5 months before EOS in order to predict end of growing season. Furthermore, they suggested that precipitation amounts, and the number of solar hours may be used to improve the predictions.

Delpierre *et al.* (2009) analysed the timing of the start of leaf coloration for temperate forests in France. It was suggested that the timing of leaf coloration might be triggered by daylength but that this might be influenced by an accumulated temperature sum to reflect the start of freezing temperatures. Hence, this was also a relatively complicated model. Estrella and Menzel (2006) analysed the timing of autumn leaf coloration for four different deciduous tree species in Germany 1951–2003. They concluded that relatively high air temperatures during August and September delayed leaf coloration while high air temperatures during May and June made leaf coloration occur earlier. However, their overall conclusion was that at present there are no robust models to

predict the onset of autumn leaf coloration.

In conclusion, the results in the present study show that the onset of the leaf budburst of Birch forests during spring in Sweden and Finland may be predicted using an accumulated air temperature sum above 5°C. The prediction was much better compared to the results with the "latitude model" currently used in the Mapping Manual (UNECE 2017). Thus, the new method developed in this study provided a more accurate representation of interannual variability in budburst for birch in Sweden and Finland, also improving the responsiveness to e.g. climate change.

Regarding the timing for the onset of the autumn leaf coloration for Birch in Finland and Sweden, a prediction model based on different meteorological parameters could not be obtained. Hence, the method currently used in the Mapping Manual (UNECE 2017) based on site latitude is suggested to remain.

Critical phenological stages for wheat and potato

The latitude model suggested in the Mapping Manual (LRTAP 2017) to estimate the date of anthesis worked very well for spring wheat but the DOY for anthesis in winter wheat was systematically overestimated by on average 13 days, with larger differences at higher latitudes and smaller at lower latitudes. Thus, the statement by the Mapping Manual that the latitude model can be used equally well for spring and winter wheat was not supported in this study. However, by reparameterization of the latitude function, separately for spring wheat and winter wheat, it was able to predict the average day of anthesis from latitude with high accuracy for both wheat types.

For potato the critical stages of planting and tuber initiation were consistent with indications of positive relationships with latitude for seven counties in south Sweden, having extensive potato cultivation and providing useful data. It can be noted that the duration of the period between planting and tuber initiation, 54 days on average, was substantially larger than the average 32 days reported from a number of experiments in different parts of Europe by Hacour *et al.* (2002).

The information provided about the critical phenological stages for Swedish conditions should facilitate accurate yield loss estimates for wheat and potato, based on the methods of the Mapping Manual (UNECE 2017), to estimate yield loss from ozone exposure, in Sweden. In addition, the analysis of the latitude model to estimate anthesis in wheat may support future revisions of the Mapping Manual and suggest the use of separate latitude functions for spring and winter wheat based on data from several countries in Europe.

The results obtained in the present study regarding methods to estimate the O_3AP for forests and agricultural crops could probably be applied for other northern European countries with similar climate conditions and similar forest and agricultural management. However, the exact parameterizations should be validated against local measurements of forest canopy gas exchange, phenological observations and agricultural statistics.

Summary and conclusions

The methods for how to estimate the yearly ozone uptake accumulation periods for Swedish forests and agricultural crops were in several cases considerably improved, compared to the methods currently used in the Mapping Manual (UNECE 2017). A novel method was developed for how to estimate the timing of the year when the stomata of boreal, evergreen, coniferous forests are potentially open, allowing for uptake of ozone to the leaf interior. The method assumed that if forest canopy net ecosystem exchange (NEE) is negative (i.e. a CO_2 removal from the atmosphere to the canopy) then canopy photosynthesis must be higher than ecosystem respiration and the stomata must be at least partially open. The timing the start of a persistent, negative NEE could be related to the timing of when the 24h mean air temperature was persistently above a threshold value.

The timing of the year for the budburst of deciduous forests could be estimated based on phenological observations from Sweden and Finland in combination with the site-specific air temperature sum, when the 24h mean air

temperatures accumulated above 5°C, since the beginning of the year exceed a threshold value, 45 degree-days. However, the onset of autumn leaf coloration could not be related to meteorological parameters and had to be related to the site latitude, the method that is already used in the Mapping Manual.

The latitude model of the Mapping Manual worked well for spring wheat but resulted in a strong bias for winter wheat, although applicable for both wheat types according to the manual. Calibrating the latitude model for best fit with observed data in this study, separately for spring and winter wheat, resulted in strong and consistent relationships between observed and modelled DOY of wheat anthesis. For potato the critical stages of planting and tuber initiation showed positive relationships with latitude.

By refining existing models, integrating region-specific climatic data and utilizing phenological observations, we may improve estimates of POD, resulting in a more accurate understanding of ozone impacts on boreal and northern temperate vegetation. Furthermore, correct estimates of yearly periods with canopy gas exchange may be useful for other applications such as modelling net ecosystem exchange.

Future research should focus on refining estimates of autumn phenology and expanding agricultural datasets to further improve ozone flux calculations and risk assessments for Northern European forests and crops.

Acknowledgements: This study was financed by the Swedish Environmental Protection Agency. We would like to thank Anders Arvidsson, Alf Djurberg and Rebecka Östlund at the Swedish Board of Agriculture for providing phenological information about the timing of developmental stages for autumn and spring wheat in Sweden. We also would like to thank Lisa Andrae (Rådhuset Nordfalan), Lars Danielsson (Tuber-Ad), Åsa Rölin (Potatiskonsult AB), Henrik Knutsson (Lyckeby) and Rebecka Östlund for providing information about the timing of developmental stages for potato. Furthermore, we would like to thank ICOS-Sweden, Jutta Holst, Department of Physical Geography and Ecosystem Science, Lund University for providing data regarding NEE for the forest sites in Sweden. Finally, we would like to thank Magnuz Engardt at the Swedish Hydrological and Meteorological Institute (SMHI) for providing 24h mean temperatures for the phenological observation sites in Finland.

Supplementary Information: The supplementary information related to this article is available online at: https://doi.org/10.60910/ber2026.bjng-4520

References

Breda N. & Granier A. 1996. Intra- and interannual variations of transpiration, leaf area index and radial growth of a sessile oak stand (Quercus petraea). *Annals of Forest Science* 53: 521–536, https://doi.org/10.1051/forest:19960232.

Delpierre N., Dufrene E., Soudani K., Ulrich U., Cecchini S., Boe J. & Francois C. 2009. Modelling interannual and spatial variability of leaf senescence for three deciduous tree species in France. *Agricultural and Forest Meteorology* 149: 938–948, https://doi.org/10.1016/j.agrformet.2008.11.014.

Emberson L.D., Ashmore M.R., Cambridge H.M., Simpson D. & Tuovinen J.P. 2000. Modelling stomatal ozone flux across Europe. *Environmental Pollution* 109: 403–413, https://doi.org/10.1016/S0269-7491(00)00043-9.

Emberson L. 2020. Effects of ozone on agriculture, forests and grasslands. *Philosophical Transactions of the Royal Society A* 78: 20190327, https://doi.org/10.1098/rsta.2019.0327.

Estiarte M. & Penuelas J. 2015. Alteration of the phenology of leaf senescence and fall in winter deciduous species by climate change: effects on nutrient proficiency. *Global Change Biology* 21: 1005–1017, https://doi.org/10.1111/gcb.12804.

Estrella N. & Menzel A. 2006. Responses of leaf colouring in four deciduous tree species to climate and weather in Germany. *Climate Research* 32: 253–267, https://doi.org/10.3354/cr032253.

Flynn D.F.B. & Wolkovich E.M. 2018. Temperature and photoperiod drive spring phenology across all species in a temperate forest community. *New Phytologist* 219: 1353–1362, https://doi.org/10.1111/nph.15232.

Fu Y.H., Zhang X., Piao S., Hao F., Geng X., Vitasse Y., Zohner C., Peñuelas J. & Janssens I.A. 2018. Daylength helps temperate deciduous trees to leaf-out at the optimal time. *Global Change Biology* 2019, 1–9, https://doi.org/10.1111/gcb.14633.

Gill A.L., Gallinat A.S., Sanders-DeMott R., Rigden A.J., Short Gianotti D.J., Mantooth J.A. & Templer P.H. 2015. Changes in autumn senescence in northern hemisphere deciduous trees: a meta-analysis of autumn phenology studies. *Annals of Botany* Page 1 of 14, https://doi.org/10.1093/aob/mcv055.

Grünhage L., Pleijel H., Mills G., Bender J., Danielsson H., Lehmann Y., Castell J.-F. & Bethenod O. 2012. Updated stomatal flux and flux-effect models for wheat for quantifying effects of ozone on grain yield, grain mass and protein yield. *Environmental Pollution* 165: 147–157, https://doi.org/10.1016/j.envpol.2012.02.026.

Hacour A., Craigon J., Vandermeiren K., Ojanperä K., Pleijel H., Danielsson H., Högy P., Finnan J. & Bindi M. 2002. CO2 and ozone effects on canopy development of potato crops across Europe. *European Journal of Agronomy* 17: 257–272, https://doi.org/10.1016/S1161-

0301(02)00065-5.

Häggmark L., Ivarsson K.-I., Gollvik S. & Olofsson P.-O. 2000. Mesan, an operational mesoscale analysis system. *Tellus* 52A: 2–20, https://doi.org/10.3402/tellusa.v52i1.12250.

Jiang N., Shen M., Ciais P., Campioli M., Peñuelas J., Körner C., Cao R., Piao S., Liu L., Wang S., Liang E., Delpierre N., Soudani K., Rao Y., Montagnani L., Hörtnag L., Paul-Limoges E., Myneni R., Wohlfahrt G., Fu Y., Šigut L., Varlagin A., Chen J., Tang Y. & Zhao W. 2022. Warming does not delay the start of autumnal leaf coloration but slows its progress rate. *Global Ecology and Biogeography* 31: 2297–2313, https://doi.org/10.1111/geb.13581.

Karlsson P.E., Braun S., Broadmeadow M., Elvira S., Emberson L., Gimeno B.S., Le Thiec D., Novak K., Oksanen E., Schaub M., Uddling J. & Wilkinson M. 2007. Risk assessments for forest trees — the performance of the ozone flux versus the AOT concepts. *Environmental Pollution* 146: 608–616, https://doi.org/10.1016/j.envpol.2006.06.012.

Klingberg J., Karlsson P.E., Andersson C., Engardt M., Pihl Karlsson G. & Pleijel H. 2019. Observed annual surface ozone maxima and minima in northern and central Europe from 1990–2015 – latitude dependence and temporal trends. *Boreal Environment Research* 24: 201–214, https://doi.org/10.60910/mk8y-9utg.

Kloos S., Klosterhalfen A., Knohl A. & Menzel A. 2024. Decoding autumn phenology: unraveling the link between observation methods and detected environmental cues. *Global Change Biology* 30, e17231, https://doi.org/10.1111/gcb.17231.

Keskitalo J., Bergquist G., Gardeström P. & Jansson S. 2005. A cellular timetable of autumn senescence. *Plant Physiology* 139: 1635–1648, https://doi.org/10.1104/pp.105.066845.

Lagergren F., Lindroth A., Dellwik E., Ibrom A., Lankreijer H., Launiainen S., Mölder M., Kolari P., Pilegaard K. & Vesala T. 2008. Biophysical controls on CO2 fluxes of three northern forests based on long-term eddy covariance data. *Tellus* 60B: 143–152, https://doi.org/10.1111/j.1600-0889.2007.00324.x.

Liu Q., Fu Y.H., Zeng Z., Huang, Li M.X. & Piao S. 2016. Temperature, precipitation, and insolation effects on autumn vegetation phenology in temperate China. *Global Change Biology* 22: 644–655, https://doi.org/10.1111/gcb.13081.

Meier U. (ed.) 2001. *Growth stages of mono and dicotyledonous plants, BBCH monograph.* Federal Biological Research Centre for Agriculture and Forestry.

Mills G., Pleijel H., Braun S., Büker P., Bermejo V., Calvo E., Danielsson H., Emberson L., González Fernández I., Grünhage L., Harmens H., Hayes F., Karlsson P.E. & Simpson D. 2011. New stomatal flux-based critical levels for ozone effects on vegetation. *Atmospheric Environment* 45: 5064–5068, https://doi.org/10.1016/j.atmosenv.2011.06.009.

Pleijel H., Danielsson H., Gelang J., Sild E. & Selldén G. 1998. Growth stage dependence of the grain yield response to ozone in spring wheat (Triticum aestivum L.). *Agriculture, Ecosystems and Environment* 70: 61–68, https://doi.org/10.1016/S0167-8809(97)00167-9.

Pleijel H., Danielsson H., Emberson L., Ashmore M. & Mills G. 2007. Ozone risk assessment for agricultural crops in Europe: further development of stomatal flux and flux–response relationships for European wheat and potato. *Atmospheric Environment* 41: 3022–3040, https://doi.org/10.1016/j.atmosenv.2006.12.002.

Pleijel H., Broberg M.C., Uddling J. & Mills G. 2018. Current surface ozone concentrations significantly decrease wheat growth, yield and quality. *Science of the Total Environment* 613–614: 687–692, https://doi.org/10.1016/j.scitotenv.2017.09.111.

Pleijel H., Danielsson H. & Broberg M.C. 2022. Benefits of the phytotoxic ozone dose (POD) index in dose-response functions for wheat yield loss. *Atmospheric Environment* 268, 118797, https://doi.org/10.1016/j.atmosenv.2021.118797.

Poikolainen J., Tolvanen A., Karhu J. & Kubin E. 2016. Seventeen-year trends in spring and autumn phenophases of Betula pubescens in a boreal environment. *International Journal of Biometeorology* 60: 1227–1236, https://doi.org/10.1007/s00484-015-1118-3.

Rousi M. & Pusenius J. 2005. Variations in phenology and growth of European white birch (Betula pendula) clones. *Tree Physiology* 25: 201–210, https://doi.org/10.1093/treephys/25.2.201.

Soja G., Barnes J., Posch M., Vandermeiren K., Pleijel H. & Mills G. 2000. Phenological weighting of ozone exposures in the calculation of critical levels for wheat, bean and plantain. *Environmental Pollution* 109: 517–524, https://doi.org/10.1016/S0269-7491(00)00055-5.

Tanja S., Berninger F., Vesala T., Markkanen T., Hari P., Mäkela A., Ilvisniemi H., Hänninen H., Nikinmma E., Huttula T., Laurila T., Aurela M., Grelle A., Lindroth A., Arneth A., Shibistova O. & Lloyd J. 2003. Air temperature triggers the recovery of evergreen boreal forest photosynthesis in spring. *Global Change Biology* 9: 1410–1426, https://doi.org/10.1046/j.1365-2486.2003.00597.x.

Templ B., Koch E., Bolmgren K., Ungersböck M., Paul A., Scheifinger H., Rutishauser T., Busto M., Chmielewski F.-M., Hájková L., Hodzić S., Kaspar F., Pietragalla B., Fresneda R.R., Tolvanen A., Vučetič V., Zimmermann K. & Zust A. 2018. Pan European phenological database (PEP725): a single point of access for European data. *International Journal of Biometeorology* 62: 1109–1113, https://doi.org/10.1007/s00484-018-1512-8.

UNECE 2017. *Manual on methodologies and criteria for modelling and mapping critical loads and levels of air pollution effects, risks and trends.* UNECE Convention on Long-range Transboundary Air Pollution. https://www.umweltbundesamt.de/system/files/medien/4038/dokumente/manual_complete_english.pdf

Vandermeiren K., Black C., Pleijel H. & De Temmerman L. 2005. Impact of rising tropospheric ozone on potato: effects on photosynthesis, growth, productivity and yield quality. *Plant, Cell and Environment* 28: 982–996, https://doi.org/10.1111/j.1365-3040.2005.01316.x.

Wallin G., Hall M., Slaney M., Räntfors M., Medhurst J. & Linder S. 2013. Spring photosynthetic recovery of boreal Norway spruce under conditions of elevated [CO2] and air temperature. *Tree Physiology* 33: 1177–1191, https://doi.org/10.1093/treephys/tpt066.

Walther S., Voigt M., Thum E., Gonsamo A., Zhang Y., Köhler P., Jung M., Arlagin A. & Guanter L. 2013. Satellite chlorophyll fluorescence measurements reveal large-scale decoupling of photosynthesis and greenness dynamics in boreal evergreen forests. *Global Change Biology* 22: 2979–2996, https://doi.org/10.1111/gcb.13200.

Zadoks J.C., Chang T.T. & Konzak C.F. 1974. A decimal code for the growth stages of cereals. *Weed Research* 14: 415–421, https://doi.org/10.1111/j.1365-3180.1974.tb01084.x.

Zohner C.M. & Renner S.S. 2015. Perception of photoperiod in individual buds of mature trees regulates leaf-out. *New Phytologist* 208: 1023–1030, https://doi.org/10.1111/nph.13510.